HHS Public Access

Author manuscript

Biochem Biophys Res Commun. Author manuscript; available in PMC 2021 April 03.

Published in final edited form as:

Biochem Biophys Res Commun. 2020 February 19; 522(4): 996–1002. doi:10.1016/j.bbrc.2019.11.164.

Equivalent L-type channel ($Ca_V1.1$) function in adult female and male mouse skeletal muscle fibers

D. Beqollari[a,1], **W.M. Kohrt**[b], **R.A. Bannister**[a,2,*]

[a]Department of Medicine - Division of Cardiology, University of Colorado School of Medicine, 12800 East 19th Avenue, P15-8006, Box 139, Aurora, CO, USA 80045

[b]Department of Medicine - Division of Geriatric Medicine, University of Colorado School of Medicine, 12631 East 17th Avenue, L15-8000 Aurora, CO, USA 80045 (303)-724-1913

Abstract

Loss of total muscle force during aging has both atrophic and non-atrophic components. The former deficit is a direct consequence of reduced muscle mass while the latter has been attributed to a depression of excitation-contraction (EC) coupling. It is well established that age-onset reductions in sex hormone production regulate the atrophic component in both males and females. However, it is unknown whether the non-atrophic component is influenced by sex hormones. Since the non-atrophic component has been linked mechanistically to reduced expression of the skeletal muscle L-type Ca^{2+} channel ($Ca_V1.1$), we recorded L-type Ca^{2+} currents, gating charge movements and depolarization-induced changes in myoplasmic Ca^{2+} from *flexor digitorum brevis* (FDB) fibers of naïve and gonadectomized mice of both sexes. Our first set of experiments sought to identify any basal differences in EC coupling or L-type Ca^{2+} flux between the sexes; no detectable differences in any of the aforementioned parameters were observed between FDB harvested from either naïve males or females. In the latter segments of the study, ovariectomy (*OVX*) and orchiectomy (*ORX*) models were used to assess the possible influence of sex hormones on EC coupling and/or L-type Ca^{2+} flux. In these experiments, FDB fibers harvested from *OVX* and *ORX* mice both showed no differences in L-type Ca^{2+} current, gating charge movement or depolarization-induced changes in Ca^{2+} release from the sarcoplasmic reticulum. Taken together, our results indicate L-type Ca^{2+} channel function and EC coupling are: 1) equivalent between the sexes, and 2) not significantly regulated by sex hormones. Since recent NIH review guidelines mandate the consideration of sex differences as a criterion for review, our work indicates the suitability of either sex for the study of the fundamental mechanisms of EC coupling. Thus, our findings may accelerate the research process by conserving animals, labor and financial resources.

[*]corresponding author (410)-706-5734 RBannister@som.umaryland.edu.

[1]Department of Surgery, University of Rochester School of Medicine and Dentistry, 601 Elmwood Avenue Box SURG, Rochester, NY, USA 14642

[2]Department of Pathology, Department of Biochemistry and Molecular Biology, University of Maryland School of Medicine, 108 North Greene Street, Room 208A, Baltimore, MD, USA 21201

Keywords

excitation-contraction coupling; sex hormones; ovariectomy; orchiectomy; $Ca_V1.1$; L-type

1. Introduction

Age-related decline in muscle force generation is a growing public health issue due to the increasing number of frailty-related accidents [1–3]. Adult humans achieve peak muscle strength in midlife and gradually lose up to 50% of muscle function by the ninth decade [4]. In this regard, sex hormones are established regulators of muscle mass and composition [5–11]. Females abruptly lose muscle force with the onset of menopause [11–14] whereas progressive muscle mass and/or force loss in males parallels decreases in testosterone levels with advancing age [7, 12].

Muscle atrophy comprises the major component of age-dependent reductions in total force generation [9, 15], but the loss of mass fails to account for the total decrement [16]. This non-atrophic component, the specific force, is revealed when the total is normalized by mass or cross-sectional area. Work from Osvaldo Delbono's laboratory has demonstrated that a depression of excitation-contraction (EC) coupling underlies this impairment of specific force in geriatric FVB mice [17–19].

In skeletal muscle, the L-type Ca^{2+} channel ($Ca_V1.1$) serves as the voltage-sensor for EC coupling [20-22, reviewed in 23]. Upon depolarization, translocation of $Ca_V1.1$'s voltage-sensing domains cause subsequent conformational rearrangements in the channel which gate, either directly or indirectly, the type 1 ryanodine receptor resident in the membrane of the sarcoplasmic reticulum (SR); opening of the ryanodine receptor provides an avenue for the Ca^{2+} efflux from the SR which ultimately binds troponin and engages the contractile apparatus. In addition to its function as the EC coupling voltage-sensor, $Ca_V1.1$ also conducts L-type Ca^{2+} current [22]. Although the physiological significance of Ca^{2+} flux via $Ca_V1.1$ has been the subject of much debate since the 1960's, some work indicates that L-type Ca^{2+} entry maintains myoplasmic Ca^{2+} levels during repetitive activity [24, 25], augments muscle contraction [26], engages excitation-transcription coupling [25], regulates metabolism [25, 27], contributes to fiber-type differentiation [25, 28], helps to refill SR Ca^{2+} stores [24, 29] and promotes development of neuromuscular junctions [30, 31]. Moreover, knock-down of $Ca_V1.1$ in adult *tibialis anterior* fibers caused profound atrophy, though it was not been determined whether the observed atrophy was a consequence of impaired EC coupling or reduced L-type Ca^{2+} flux [32].

While the effects of sex hormones (i.e., estradiol, testosterone) on muscle mass and fiber-type composition have been fairly-well characterized [9, 11], the influence of sex hormones on the non-atrophic component of force loss in aging remain(s) largely unknown. To begin to address this knowledge gap, we compared L-type Ca^{2+} currents, charge movement, and changes in myoplasmic Ca^{2+} recorded from *flexor digitorum brevis* (FDB) muscle fibers harvested from mice of both sexes and from gonadectomized mice.

2. Materials and methods

2.1 Mice

All procedures involving C57BL/6 mice were approved by the University of Colorado-Anschutz Medical Campus Institutional Animal Care and Use Committee (91813(05)1D) and were in line with the National Institutes of Health guidelines on laboratory animal research. All mice were purchased from Charles River Laboratories, Wilmington, MA. Orchiectomy male ($N = 5$), ovariectomy female ($N = 4$), and respective age-matched C57BL/6J mice [(male ($N = 6$) and female ($N = 4$)], were used during the course of this study. The gonadectomies were performed by Charles River Laboratories personnel at 13 weeks of age. One month later (i.e., at 17 weeks), mice were euthanized via isoflurane overdose followed by cervical dislocation at the University of Colorado-Anschutz Medical Campus.

2.2 Muscle fiber preparation

FDB muscles were dissociated as described previously [33].

2.3 Electrophysiology and whole-cell recordings of myoplasmic Ca^{2+} transients

Borosilicate patch pipettes had resistances of ≤1.0 MΩ when filled with internal solution, which consisted of (mM): 140 Cs-aspartate, 10 Cs_2-EGTA, 5 $MgCl_2$, and 10 HEPES, pH 7.4 with CsOH. To record changes in intracellular Ca^{2+}, the pentapotassium salt of Fluo 3 single wavelength Ca^{2+} indicator dye (Invitrogen) was added to the standard internal solution for a final concentration of 200 μM. The bath contained (mM): 145 TEA-methanesulfonic acid, 10 $CaCl_2$, 10 HEPES, 2 $MgSO_4$, 1 4-aminopyridine, 0.1 anthracene-9-carboxylic acid, 0.002 TTX, pH 7.4 with TEA-OH. 10 μM *N*-benzyl-*p*-tolunesulfonamide (Sigma Aldrich, St. Louis, MO) was added to the external solution for all experiments to prevent movement artifacts. Following the establishment of the whole-cell configuration, the dye was allowed to diffuse into the cell interior for no less than 20 minutes. A 100 W mercury illuminator and a set of fluorescein filters were used to excite the dye. A computer-controlled shutter was used to block illumination in the intervals between test potentials. Fluorescence emission was measured by means of a fluorometer apparatus (Biomedical Instrumentation Group, University of Pennsylvania). Fluorescence data are expressed as ΔF/F, where ΔF represents the change in peak fluorescence from baseline during the test pulse and F is the fluorescence immediately prior to the test pulse minus the average background fluorescence. The peak value of the fluorescence change (ΔF/F) for each test potential (V) was fitted according to:

$$(\Delta F/F) = (\Delta F/F)_{max}/\{1 + \exp[(V_F - V)/k_F]\}, \quad (1)$$

where $(\Delta F/F)_{max}$ is the maximal fluorescence change, V_F is the potential causing half the maximal change in fluorescence, and k_F is a slope parameter.

L-type Ca^{2+} currents were recorded with the same external solution used to record myoplasmic Ca^{2+} transients described above. 1 mM $LaCl_3$ and 0.5 mM $CdCl_2$ were added when recording charge movements. Linear components of leak and capacitive current were corrected with -P/4 online subtraction protocols. Output filtering was at 2–5 kHz and

digitization was either at 5 kHz (currents) or 10 kHz (charge movements). Cell capacitance (C_m) was determined by integration of a transient from −80 mV to −70 mV using Clampex 10.3 (Molecular Devices). The average value of C_m for all fibers used in the study was 2.02 ± 0.05 nF (n = 104 fibers). The time constant for the decay of the whole-cell capacity transient was reduced as much as possible using the analog compensation circuit of the amplifier; the average values of τ_m and R_a were 958 ± 6 μs and 528 ± 16 kΩ, respectively. Current-voltage (I-V) curves were fitted according to:

$$I = G_{max}*(V-V_{rev})/\{1+\exp[-(V-V_{1/2})/k_G]\}, \quad (2)$$

where I is the normalized current for the test potential V, V_{rev} is the reversal potential, G_{max} is the maximum channel conductance, $V_{1/2}$ is the half-maximal activation potential and k_G is the slope factor. For charge movements, Q_{ON}-V relationships were fitted according to:

$$QoN = Q_{max}/\{1+\exp[(V_Q - V)/k_Q]\}, \quad (3)$$

where Q_{max} is the maximal Q_{ON}, V_Q is the potential causing movement of half the maximal charge, and k_Q is a slope parameter. All experiments were performed ~25° C.

2.4 Analysis

All data are presented as mean ± SEM. All statistical comparisons were made by two-tailed, unpaired t-test with $P < 0.05$ considered significant. Figures were made using SigmaPlot (version 11.0, SSPS Inc. San Jose, CA).

3. Results

3.1 $Ca_V1.1$ function is equivalent in male and female FDB fibers

To determine whether there are clear differences in EC coupling between sexes, we assessed changes in intracellular Ca^{2+} in response to depolarization in FDB fibers harvested from four month-old male and female C57BL/6 mice. In this experiment, Ca^{2+} transients for female and male FDB fibers were found to be similar in amplitude (Fig. 1A-B). Peak fluorescence changes were 3.3 ± 0.5 ΔF/F for female and 3.0 ± 0.5 ΔF/F for male fibers (both n = 6; P = 0.738; Fig. 1C; Table 1). Recordings of L-type current from female and male FDB fibers also showed no differences in $Ca_V1.1$ channel function between the sexes (Fig. 1D-E). L-type current densities at the peaks of the I-V relationships (i.e., +10 mV) were −10.8 ± 0.9 pA/pF for female (n = 11) and −11.1 ± 1.3 pA/pF for male (n = 8) fibers (P = 0.843; Fig. 1F). Likewise, maximal charge movement was indistinguishable between male and female fibers (Fig. 1G-H). Maximal charge movement registered 34.7 ± 1.8 nC/μF for female (n = 11) and 35.0 ± 1.2 nC/μF for male (n = 9) fibers (P = 0.890; Fig. 1I; Table 2).

3.2 $Ca_V1.1$ function is little affected by ovariectomy

We next utilized FDB fibers obtained from ovariectomized (*OVX*) mice to investigate whether loss of ovarian function impacts EC coupling and/or L-type channel activity. One month post-procedure, there was a non-significant trend towards an increase in mass for the *OVX* group relative to the naïve female control group (25.52 ± 1.50 g *vs.* 23.86 ± 1.37 g, respectively, both N = 4; $P > 0.05$). There were virtually no discernable differences in Ca^{2+}

transient amplitude between control female and *OVX* fibers (3.3 ± 0.8 ΔF/F for *OVX*, $n = 7$; $P = 0.970$ *vs.* control female; Fig. 2A-B; Table 1). Peak current densities were also unchanged ($I_{dens} = -10.0 \pm 1.2$ pA/pF, $n = 7$ for *OVX* fibers; $P = 0.569$ *vs.* control female; Fig. 2C-D). Consistent with these observations, control female and *OVX* fibers had similar charge movement ($Q_{max} = 33.7 \pm 1.6$ nC/μF, $n = 7$ for *OVX* fibers; $P = 0.707$ *vs.* control female; Fig. 2E-F; Table 2), though a significantly different slope factor in the Q-V relationship was evident ($P = 0.035$; Table 2).

3.3 $Ca_V1.1$ function is unaltered in mice with orchiectomy

Age-related declines in muscle force consequential to lower testosterone production are well documented. However, a role for testicular function in the maintenance EC coupling and/or $Ca_V1.1$ channel function has not been described. To address this knowledge gap, we investigated whether myoplasmic Ca^{2+} transients, L-type current and/or charge movement were affected by orchiectomy (*ORX*). One month post-procedure, *ORX* males were found to be lighter than naïve control males (24.42 ± 0.68 g, $N = 5$ *vs.* 28.22 ± 1.30 g, $N = 6$, respectively; $P < 0.05$). Control male and *ORX* fibers both displayed robust Ca^{2+} transients upon depolarization (compare Fig. 3A with Fig. 1B). Peak fluorescence amplitudes at were similar betwixt control male and *ORX* fibers (3.2 ± 0.3 ΔF/F, $n = 8$; $P = 0.817$ *vs.* control male; Fig. 3C; Table 1). As illustrated by the representative L-type currents shown in Figure 3D and 1B, there were no differences in L-type current density between control male and *ORX* fibers, respectively ($I_{dens} = -10.4 \pm 0.9$ pA/pF, $n = 13$ for *ORX* fibers; $P = 0.641$ *vs.* control male; Fig. 3F). Maximal charge movement was similar between control male and *ORX* groups (35.7 ± 2.0 nC/μF, $n = 12$ for *ORX* fibers; $P = 0.777$ *vs.* control male; Fig. 3E-F; Table 2).

4. Discussion

Although there is some information available on how sex hormones affect cardiac EC coupling in rodents [34–36], the current study offers the first direct investigation of sex differences in skeletal muscle. To this end, our results indicate L-type channel function and EC coupling are: 1) not different between the sexes (Fig. 1), and 2) not significantly affected by gonadectomy (Figs. 2 and 3). Our findings are significant because earlier studies found that both ovariectomized and orchiomectomized mice generated lower specific force than naïve female and male mice, respectively [*cf.* 37]. Likewise, testosterone and estrogens have both been found to influence specific force in humans and in rodents [9, 11, 38, 39]. Thus, our results suggest these differences in specific force generation are unrelated to regulation of the EC coupling macromolecular signaling complex.

One confounding aspect of our study is the comparison between humans and mice wherein the *ORX* and *OVX* models likely do not reproduce human age-dependent loss of hormones with fidelity. Unfortunately, this comparative strategy is necessary as the performance of such experiments with living human tissue is generally not feasible. Moreover, the mice used in this study were not geriatric and thus the effects of age-dependent modifiers of sex hormone signaling were absent. Another reason for the lack of effect could be a consequence of the preparation in that mouse FDB muscles are comprised of ~95% Type

IIA, B and X fast-twitch glycolytic fibers [40]. The lack of effect of gonadectomy in both *OVX* and *ORX* mice may reflect the possibility that Type IIA and Type IIX fibers are more resistant to EC uncoupling than Type I slow-twitch oxidative fibers, though earlier work indicates that substantial EC uncoupling occurs in geriatric FDB fibers [19].

While no significant differences in EC coupling were observed between male and female mice and neither ovariectomy nor orchiectomy influenced L-type current amplitude, charge movement or myoplasmic Ca^{2+} release, the impact of the current study extends beyond the raw scientific value of these observations. Specifically, our work indicates the suitability of either sex for the study of L-type channel biophysics and EC coupling in skeletal muscle. Since recent NIH review guidelines mandate assessment of differences between the sexes as a criteria for review (please see https://grants.nih.gov/grants/peer/guidelines_general/Reviewer_Guidance_on_Rigor_and_Transparency.pdf), our findings may accelerate the research process by conserving animals, labor and financial resources.

Acknowledgements

We thank Drs. U. Meza, D. Oskar and S. Papadopoulos for comments on early versions of the manuscript. This work was supported by grants from NICHD (HD073063 to W.M.K.), the Colorado CTSI (to D.B.) and NINDS (NS103777 to R.A.B.).

Abbreviations

EC	excitation-contraction
FDB	*flexor digitorum brevis*
ORX	orchiectomy
OVX	ovariectomy
SR	sarcoplasmic reticulum

References

[1]. Khaw KT, Epidemiological aspects of ageing. Philos. Trans. R. Soc. Lon.d B. Biol. Sci 352 (1997) 1829–1835.

[2]. Fuller GF, Falls in the elderly. Am. Fam. Physician 61 (2000) 2159–2168. [PubMed: 10779256]

[3]. Runge M, Hunter G, Determinants of musculoskeletal frailty and the risk of falls in old age. J Musculoskelet Neuronal Interact. 6 (2006) 167–173. [PubMed: 16849828]

[4]. Jasuja R, LeBrasseur NK, Regenerating skeletal muscle in the face of aging and disease. Am. J. Phys. Med. Rehabil 93 (2014) S88–S96. [PubMed: 24879554]

[5]. Sipilä S, Taaffe DR, Cheng S, et al., Effects of hormone replacement therapy and high-impact physical exercise on skeletal muscle in post-menopausal women: a randomized placebo-controlled study. Clin. Sci. (Lond) 101 (2001) 147–157. [PubMed: 11473488]

[6]. Taaffe DR, Newman AB, Haggerty CL, et al., Estrogen replacement, muscle composition, and physical function: the Health ABC Study. Med. Sci. Sports. Exerc 37 (2005) 1741–1747. [PubMed: 16260975]

[7]. Ottenbacher KJ, Ottenbacher ME, Ottenbacher AJ, et al., Androgen treatment and muscle strength in elderly men: a meta-analysis. J. Am. Geriatr. Soc 54 (2006) 1666–7163. [PubMed: 17087692]

[8]. Ronkainen PH, Kovanen V, Alén M, et al., Postmenopausal hormone replacement therapy modifies skeletal muscle composition and function: a study with monozygotic twin pairs. J. Appl. Physiol 107 (2009) 25–33. [PubMed: 19246654]

[9]. Haizlip KM, Harrison BC, Leinwand LA, Sex-based differences in skeletal muscle kinetics and fiber-type composition. Physiology 30 (2015) 30–39. [PubMed: 25559153]

[10]. De Spiegeleer A, Beckwée D, Bautmans I, et al., Pharmacological interventions to improve muscle mass, muscle strength and physical performance in older people: an umbrella review of systematic reviews and meta-analyses. Sarcopenia Guidelines Development group of the Belgian Society of Gerontology and Geriatrics (BSGG). Drugs Aging 35 (2018) 719–734. [PubMed: 30047068]

[11]. Collins BC, Laakkonen EK, Lowe DA, Aging of the musculoskeletal system: how the loss of estrogen impacts muscle strength. Bone 123 (2019) 137–144. [PubMed: 30930293]

[12]. Phillips SK, Rook KM, Siddle NC, et al., Muscle weakness in women occurs at an earlier age than in men, but strength is preserved by hormone replacement therapy. Clin. Sci. (Lond) 84 (1993) 95–98. [PubMed: 8382141]

[13]. Samson MM, Meeuwsen IB, Crowe A, et al., Relationships between physical performance measures, age, height and body weight in healthy adults. Age Ageing 29 (2000) 235–242. [PubMed: 10855906]

[14]. Enns DL, Tiidus PM, The influence of estrogen on skeletal muscle: sex matters. Sports Med. 40 (2010) 41–58. [PubMed: 20020786]

[15]. Kent-Braun JA, Ng AV, Specific strength and voluntary muscle activation in young and elderly women and men. J. Appl. Physiol 87 (1999) 22–29. [PubMed: 10409554]

[16]. Lynch NA, Metter EJ, Lindle RS, et al., Muscle quality. I. Age-associated differences between arm and leg muscle groups. J. Appl. Physiol 86 (1999) 188–194. [PubMed: 9887130]

[17]. Delbono O, O'Rourke KS, Ettinger WH, Excitation-calcium release uncoupling in aged single human skeletal muscle fibers. J. Membr. Biol 148 (1995) 211–222. [PubMed: 8747553]

[18]. Renganathan M, Messi ML, Delbono O, Overexpression of IGF-1 exclusively in skeletal muscle prevents age-related decline in the number of dihydropyridine receptors. J. Biol. Chem 273 (1998) 28845–28851.

[19]. Wang ZM, Messi ML, Delbono O, L-type Ca^{2+} channel charge movement and intracellular Ca^{2+} in skeletal muscle fibers from aging mice. Biophys. J 78 (2000) 1947–1954. [PubMed: 10733973]

[20]. Schneider MF, Chandler WK, Voltage dependence charge movement in skeletal muscle: a possible step in excitation-contraction coupling. Nature 242 (1973) 244–246. [PubMed: 4540479]

[21]. Ríos E, Brum G, Involvement of dihydropyridine receptors in excitation-contraction coupling in skeletal muscle. Nature 325 (1987) 717–720. [PubMed: 2434854]

[22]. Tanabe T, Beam KG, Powell JA, et al., Restoration of excitation-contraction coupling and slow calcium current in dysgenic muscle by dihydropyridine receptor complementary DNA. Nature 336 (1988) 134–139. [PubMed: 2903448]

[23]. Bannister RA, Bridging the myoplasmic gap II: more recent advances in skeletal muscle EC coupling. J. Exp. Biol 219 (2016) 175–182. [PubMed: 26792328]

[24]. Cherednichenko G, Hurne AM, Fessenden JD, et al., Conformational activation of Ca^{2+} entry by depolarization of skeletal myotubes. Proc. Natl. Acad. Sci. U.S.A 101 (2004) 15793–15798.

[25]. Lee CS, Dagnino-Acosta A, Yarotskyy V, et al., Ca2+ permeation and/or binding to CaV1.1 fine-tunes skeletal muscle Ca2+ signaling to sustain muscle function. Skelet. Muscle 5 (2015) 4. [PubMed: 25717360]

[26]. Mosca B, Delbono O, Messi ML, et al., Enhanced dihydropyridine receptor calcium channel activity restores muscle strength in JP45/CASQ1 double knockout mice. Nat. Commun 4 (2013) 1541. [PubMed: 23443569]

[27]. Georgiou DK, Dagnino-Acosta A, Lee CS, et al., Ca^{2+} binding/ permeation via calcium channel, $Ca_V1.1$, regulates the intracellular distribution of the fatty acid transport protein, CD36, and fatty acid metabolism. J. Biol. Chem 290 (2015) 23751–23765.

[28]. Sultana N, Dienes B, Benedetti A, et al., Restricting calcium currents is required for correct fiber type specification in skeletal muscle. Development 143 (2016) 1547–1559. [PubMed: 26965373]

[29]. Robin G, Allard B, Voltage-gated Ca^{2+} influx through L-type channels contributes to sarcoplasmic reticulum Ca^{2+} loading in skeletal muscle. J. Physiol 593 (2015) 4781–4797. [PubMed: 26383921]

[30]. Chen F, Liu Y, Sugiura Y, et al., Neuromuscular synaptic patterning requires the function of skeletal muscle dihydropyridine receptors. Nat. Neurosci 14 (2011) 570–577. [PubMed: 21441923]

[31]. Kaplan MM, Sultana N, Benedetti A, et al., Calcium influx and release cooperatively regulate AChR patterning and motor axon outgrowth during neuromuscular junction formation. Cell Rep. 23 (2018) 3891–3904. [PubMed: 29949772]

[32]. Piétri-Rouxel F, Gentil C, Vassilopoulos S, et al., DHPR α_{1S} subunit controls skeletal muscle mass and morphogenesis. EMBO J. 29 (2010) 643–654. [PubMed: 20033060]

[33]. Beqollari D, Romberg CF, Filipova D, et al., Rem uncouples excitation-contraction coupling in mouse skeletal muscle fibers. J. Gen. Physiol 146 (2015) 97–108. [PubMed: 26078055]

[34]. Grandy SA, Howlett SE, Cardiac excitation-contraction coupling is altered in myocytes from aged male mice but not in cells from aged female mice. Am. J. Physiol. Heart. Circ. Physiol 291 (2006) H2362-H2370.

[35]. Howlett SE, Age-associated changes in excitation-contraction coupling are more prominent in ventricular myocytes from male rats than in myocytes from female rats. Am. J. Physiol. Heart Circ. Physiol 298 (2010) H659–H670. [PubMed: 19966062]

[36]. MacDonald JK, Pyle WG, Reitz CJ, Howlett SE, Cardiac contraction, calcium transients, and myofilament calcium sensitivity fluctuate with the estrous cycle in young adult female mice. Am. J. Physiol. Heart Circ. Physiol 306 (2014) H938–H953. [PubMed: 24464757]

[37]. Ueberschlag-Pitiot V, Stantzou A, Messéant J, et al., Gonad-related factors promote muscle performance gain during postnatal development in male and female mice. Am. J. Physiol. Endocrinol. Metab 313 (2017) E12–E25. [PubMed: 28351832]

[38]. Chan S, Head SI, Age- and gender-related changes in contractile properties of non-atrophied EDL muscle. PLoS One 5 (2010) e12345.

[39]. Lamboley CR, Xu H, Dutka TL, et al., Effect of androgen deprivation therapy on the contractile properties of type I and type II skeletal muscle fibres in men with non-metastatic prostate cancer. Clin. Exp. Pharmacol. Physiol 45 (2018) 146–154. [PubMed: 29044613]

[40]. Tarpey MD, Amorese AJ, Balestrieri NP, et al., Characterization and utilization of the flexor digitorum brevis for assessing skeletal muscle function. Skelet. Muscle 8 (2018) 14. [PubMed: 29665848]

Highlights

- Sex differences in skeletal excitation-contraction coupling were investigated.
- No differences were observed in L-current or Ca^{2+} release within males and females.
- L-channel function and EC coupling were unaffected by ovariectomy or orchiectomy.
- Our results indicate the suitability of either sex for the study of EC coupling.
- Our findings may accelerate research by conserving animals and other resources.

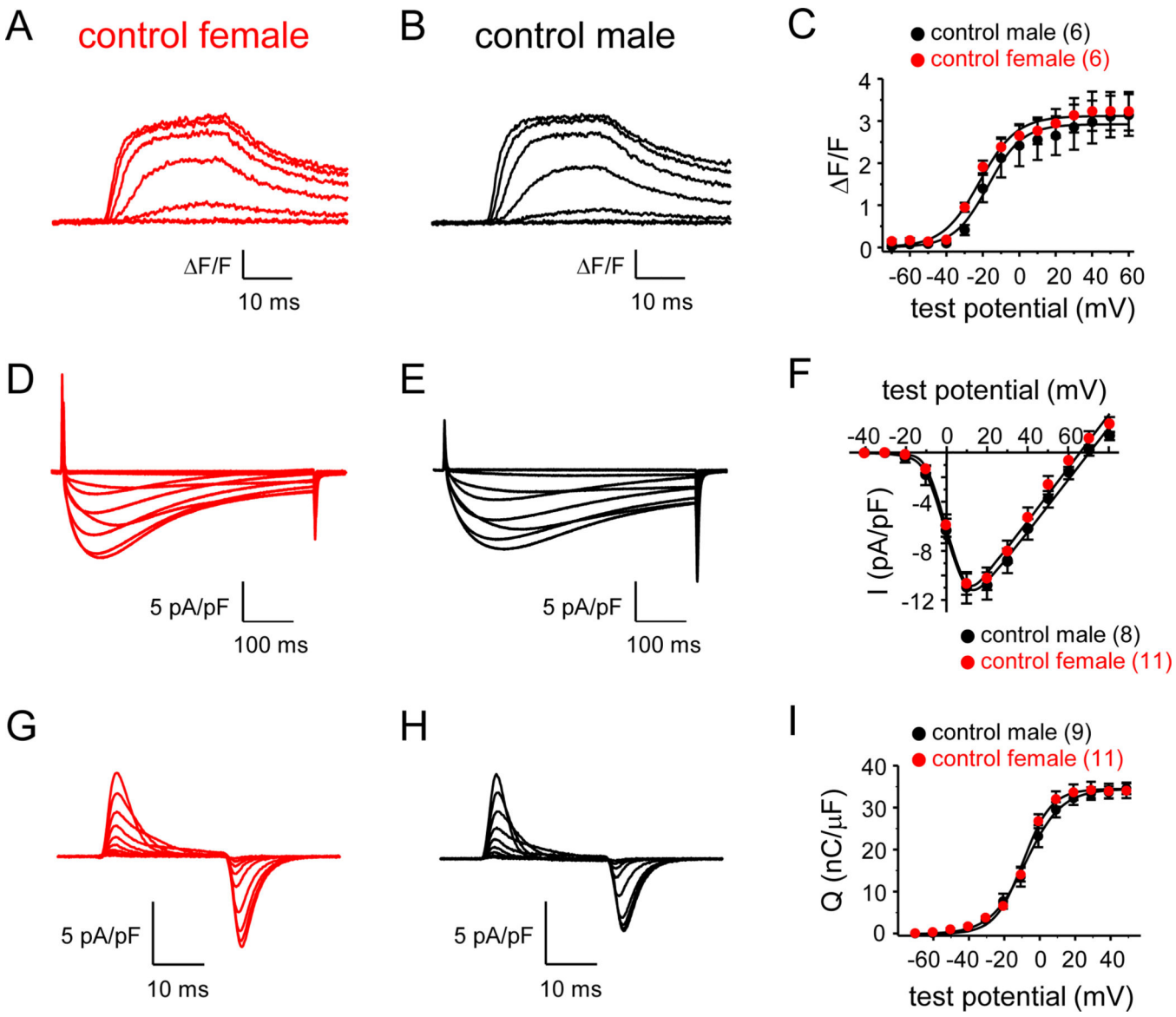

Fig. 1. Equivalent EC coupling and $Ca_V1.1$ channel function in female and male C57BL/6 FDB fibers.

Representative myoplasmic Ca^{2+} transients elicited by 25 ms depolarizations from −80 mV to −50 through +10 mV in 10 mV increments from FDB fibers harvested from age-matched, C57BL/6J female (A) and male (B) mice. The peak ΔF/F-V relationships for naïve female and male fibers are presented in panel (C). Ca^{2+} transients were evoked at 0.1 Hz by test potentials ranging from −70 mV through +60 mV in 10 mV increments. The smooth curves in panel (C) are plotted according to Eq. 1 with the respective fit parameters shown in Table 1. Representative whole-cell recordings of L-type currents elicited by 500 ms step depolarizations from −80 mV to −40 through +50 mV in 10 mV increments are shown for female (D) and male (E) fibers. (F) Peak I-V relationships corresponding to the current families shown in panels (D) and (E). Currents were evoked at 0.1 Hz by test potentials ranging from −40 mV through +80 mV in 10 mV increments. Representative recordings of charge movements elicited by 25 ms depolarizations from −80 mV to −60 through +20 mV

in 10 mV increments are shown for female (G) and male (H) fibers. (I) Q-V relationships corresponding to the charge movements shown in panels (G) and (H). Charge movements were evoked at 0.1 Hz by test potentials ranging from −70 mV through +50 mV in 10 mV increments. The smooth curves in panels (F) and (I) are plotted according to Eq. 2 and Eq. 3, respectively, with fit parameters displayed in Table 2. The numbers of analyzed fibers are indicated in parentheses. Throughout, error bars represent ±SEM.

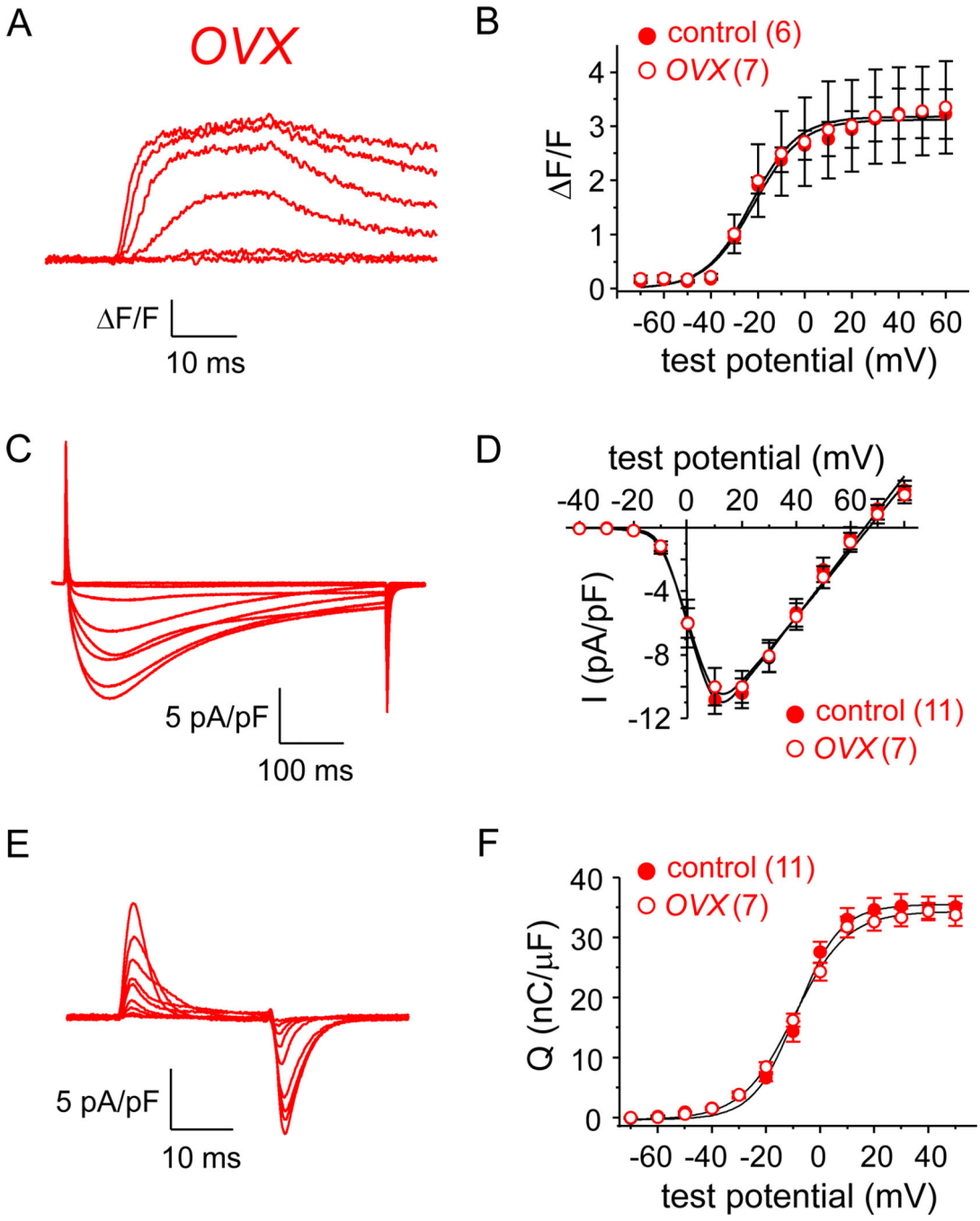

Fig. 2. EC coupling and $Ca_V1.1$ channel function in FDB fibers are little affected by ovariectomy.

Representative myoplasmic Ca^{2+} transients from an FDB fiber harvested from an *OVX* mouse (A). (B) the peak ΔF/F-V relationship for *OVX* mice ($n = 7$) is shown with that shown for control female mice in Fig. 1C. Representative whole-cell recordings of L-type currents are shown for an *OVX* fiber (C). (D) Peak I-V relationships corresponding to the current family shown in panel (C; $n = 7$) with the I-V relationship for control female mice from Fig. 1F. Representative recordings of intramembrane charge movements are shown for an *OVX* fiber (E). (F) Q-V relationships corresponding to the charge movements shown in

panel (E; $n = 11$) with the Q-V relationship for control female mice from Fig. 1I. See Figure 1 legend for protocol details.

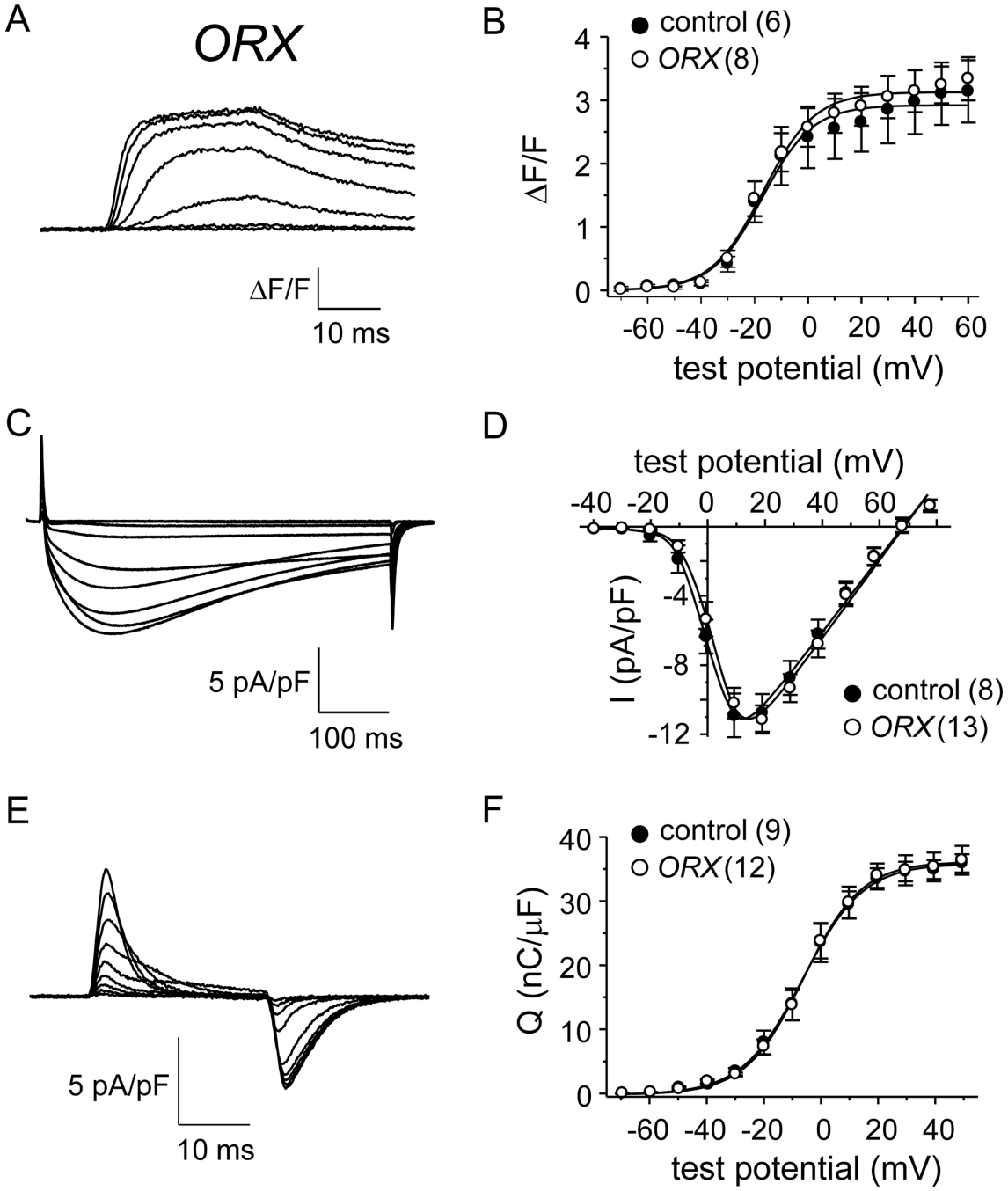

Fig. 3. EC coupling and $Ca_V1.1$ channel function in FDB fibers are little affected by orchiectomy.

Representative myoplasmic Ca^{2+} transients from an FDB fiber harvested from an *ORX* mouse (A). (B) the peak ΔF/F-V relationship for ORX mice ($n = 8$) is shown with that shown for control male mice in Fig. 1C. Representative whole-cell recordings of L-type currents are shown for an *ORX* fiber (C). (D) Peak I-V relationships corresponding to the current family shown in panel (C; $n = 13$) with the I-V relationship for control male mice from Fig. 1F. Representative recordings of charge movements are shown for an *ORX* fiber (E). (F) Q-V relationships corresponding to the charge movements shown in panel (E; $n =$

13) with the Q-V relationship for control male mice from Fig. 1I. See Figure 1 legend for protocol details.

Table 1

Ca^{2+} transient fit parameters.

	ΔF/F-V		
	$\Delta F/F_{max}$	**V_F (mV)**	**k_F (mV)**
control female	3.3 ± 0.5 (6)	9.7 ± 2.6	−20.5 ± 4.6
OVX	3.3 ± 0.8 (7)	12.8 ± 2.4	−15.5 ± 4.3
control male	3.0 ± 0.5 (6)	10.4 ± 1.7	−14.3 ± 4.1
ORX	3.2 ± 0.3 (8)	9.4 ± 1.1	−15.5 ± 2.3

Data are given as mean ±SEM, with the numbers in parentheses indicating the number of fibers tested. Data were fit by Eq. 1. The triple thin lines separate two distinct experimental groups: 1) female and 2) male. No significant differences were observed in either group or between male and female controls (all $P > 0.05$, two-tailed unpaired *t*-tests).

Table 2

Conductance and charge movement fit parameters.

	G-V				*Q-V*		
	G_{max}(nS/nF)	**$V_{1/2}$(mV)**	**V_{rev}(mV)**	**k_G(mV)**	**Q_{max}(nC/μF)**	**V_Q(mV)**	**k_Q(mV)**
control female	231.7 ± 16.8 (11)	1.3 ± 1.2	64.0 ± 2.8	4.1 ± 0.2	34.7 ± 1.8(11)	−8.7 ± 0.9	7.5 ± 0.5
OVX	214.4 ± 19.1 (7)	1.6 ± 2.2	66.6 ± 2.4	3.8 ± 0.4	33.7 ± 1.6 (7)	−9.6 ± 0.9	9.5 ± 0.6 *
control male	218.3 ± 17.8 (8)	0.7 ± 2.3	69.5 ± 1.9	4.4 ± 0.3	35.0 ± 1.2 (9)	−5.8 ± 3.2	8.7 ± 0.9
ORX	236.0 ± 15.4 (13)	3.2 ± 1.9	69.1 ± 2.1	3.6 ± 0.4	35.7 ± 2.0 (12)	−4.8 ± 2.7	8.7 ± 0.9

Data are given as mean ±SEM, with the numbers in parentheses indicating the number of fibers tested. Conductance and charge movement data were fit by Eqs. 2 and 3, respectively. As in Table 1, the triple thin lines separate two distinct experimental groups: 1) female and 2) male. No significant differences were observed between male and female controls (all $P > 0.05$, two-tailed, unpaired *t*-tests). A significant difference within the female group is indicated

*(denotes $P < 0.05$).